Differential Inhibition of Six Copper Amine Oxidases by a Family of 4-(Aryloxy)-2-butynamines: Evidence for a New Mode of Inactivation†

Kimberly M. O'Connell,‡,§ David B. Langley,‡,|| Eric M. Shepard,§ Anthony P. Duff,|| Heung-Bae Jeon,⊥ Gang Sun,⊥ Hans C. Freeman,|| J. Mitchell Guss,|| Lawrence M. Sayre,⊥ and David M. Dooley*,§

Department of Chemistry and Biochemistry, Montana State University, Bozeman, Montana 59717, School of Molecular and Microbial Biosciences, University of Sydney, Sydney, N. S. W. 2006, Australia, and Department of Chemistry, Case Western Reserve University, Cleveland, Ohio 44106

Received April 21, 2004; Revised Manuscript Received June 8, 2004

ABSTRACT: A series of compounds derived from a previously identified substrate analogue of copper amine oxidases (CuAOs) (Shepard et al. (2002) *Eur. J. Biochem.* 269, 3645−3658) has been screened against six different CuAOs with a view to designing potent and selective inhibitors. The substrate analogues investigated were 4-(1-naphthyloxy)-2-butyn-1-amine, 4-(2-methylphenoxy)-2-butyn-1-amine, 4-(3-methylphenoxy)-2-butyn-1-amine, 4-(4-methylphenoxy)-2-butyn-1-amine, and 4-phenoxy-2-butyn-1-amine. These compounds were screened against equine plasma amine oxidase (EPAO), *Pisum sativum* amine oxidase (PSAO), *Pichia pastoris* lysyl oxidase (PPLO), bovine plasma amine oxidase (BPAO), human kidney diamine oxidase (KDAO), and *Arthrobacter globiformis* amine oxidase (AGAO) to examine the effect of different substituent groups on potency. Despite the similar structures of the 4-aryloxy analogues evaluated, striking differences in potency were observed. In addition, crystal structures of AGAO derivitized with 4-(2-naphthyloxy)-2-butyn-1-amine and 4-(4-methylphenoxy)-2-butyn-1-amine were obtained at a resolution of 1.7 Å. The structures reveal a novel and unprecedented reaction mechanism involving covalent attachment of the α,β-unsaturated aldehyde turnover product to the amino group of the reduced 2,4,5-trihydroxyphenylalanine quinone (TPQ) cofactor. Collectively, the structural and inhibition results support the feasibility of designing selective mechanism-based inhibitors of copper amine oxidases.

Amine oxidases catalyze the deamination of primary amines to their corresponding aldehydes producing ammonia and hydrogen peroxide (eq 1).

$$RCH_2NH_3^+ + O_2 + H_2O \rightarrow RCHO + NH_4^+ + H_2O_2 \quad (1)$$

Amine oxidases can be divided into two groups based on the cofactors they utilize, quinone and copper-containing amine oxidases (CuAOs),[1] and flavin-dependent monoamine oxidases (MAOs). MAOs are located exclusively in the outer mitochondrial membrane of almost all cell types and can oxidize primary, secondary, and tertiary amines either by a concerted covalent catalysis or by a single electron-transfer mechanism, both requiring FAD as a cofactor (*1*). Quinone copper-containing amine oxidases generally oxidize primary amines and can be subdivided based on the cofactor present in the active site. The first group contains 2,4,5-trihydroxyphenylalanine quinone (TPQ) which is formed in a self-processing posttranslational modification of a conserved tyrosine within the sequence Ser/Thr−X_{aa}−X_{aa}−Asn−Tyr (TPQ)−Asp/Glu−Tyr/Asn. Molecular oxygen and copper are required in order for this modification to occur (*2*, *3*). The second class of quinone copper-containing amine oxidases use lysyl tyrosylquinone as their cofactor and are referred to as lysyl oxidases. Lysyl oxidases are involved in connective tissue maturation through the deamination of peptidyl lysine side chains that initiate lysine residue cross-linking in collagen and elastin (for reviews see refs 4 and 5).

Copper-containing amine oxidases can be found throughout nature and have been purified from many sources including plants, mammals, and microorganisms (*6*−*9*). In microorganisms, CuAOs play a nutritional role allowing primary amines to be used as the sole source of carbon and nitrogen. In higher organisms the physiological roles of CuAOs are not yet fully clear. In plants, it is theorized that amine oxidases aid in the biosynthesis of hormones, cell

† This work is supported by the following grants: National Institutes of Health (NIH) Grant GM27659 to D.M.D.; Australian Research Council Grant DP0208320 to H.C.F. and J.M.G.; NIH Grant GM48812 to L.M.S. and D.M.D.

* E-mail: dmdooley@montana.edu, Tel.: + 1-406-994-4371, Fax: + 1-406-994-7989.

⊥ Case Western Reserve University.

|| University of Sydney.

§ Montana State University.

‡ These authors contributed equally.

[1] Abbreviations: ABTS, 2, 2′-azino-bis(3-ethyl)-benzthiazoline-6-sulfonic acid; AGAO, *Arthrobacter globiformis* amine oxidase; BME, β-mercaptoethanol; BPAO, bovine plasma amine oxidase; CuAO, copper amine oxidase; DAO, diamine oxidase; ECAO, *Escherichia coli* amine oxidase; EPAO, equine plasma amine oxidase; HPAO, *Hansenula polymorpha* amine oxidase; HRP, horseradish peroxidase; KDAO, human kidney diamine oxidase; MAO, monoamine oxidase; NBT, nitroblue tetrazolium; PPLO, *Pichia pastoris* lysyl oxidase; PSAO, *Pisum sativum* amine oxidase; SSAO, semicarbazide-sensitive amine oxidase; TPQ, 2,4,5-trihydroxyphenylalanine quinone; TPQ_{amr}, TPQ aminoresorcinol; TPQ_{imq}, TPQ iminoquinone; TPQ_{ox}, oxidized TPQ.; TPQ_{red}, reduced TPQ.

10.1021/bi0492004 CCC: $27.50
Published on Web 08/03/2004

Scheme 1: Proposed Mechanism of Turnover for Amine Oxidases

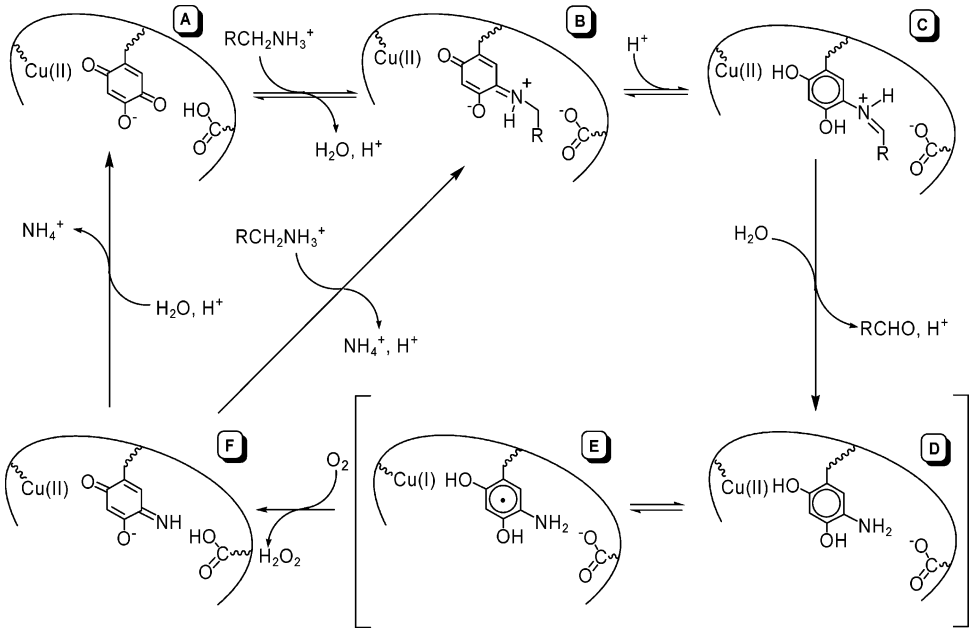

walls, and alkaloids (*10*). In mammals, function seems to be tissue specific involving physiological response to injury, apoptosis, cell growth, signaling, and detoxification (*10*). Four types of TPQ copper amine oxidases have been described from mammalian sources: plasma amine oxidase, diamine oxidase (DAO), retinal amine oxidase, and semicarbazide-sensitive amine oxidase (SSAO) (*10*). SSAO has multiple functions depending on its location, including glucose homeostasis, lymphocyte adhesion, and adipocyte maturation (*11*−*13*). It was recently discovered that human kidney diamine oxidase (KDAO) has the highest substrate specificity with 1-methylhistamine and histamine, indicating that this enzyme could play an integral but as yet undetermined role in histamine metabolism (*8*).

Five CuAO structures have been experimentally determined: *Escherichia coli* amine oxidase (ECAO) (*14*), *Pisum sativum* amine oxidase (PSAO) (*15*), *Pichia pastoris* lysyl oxidase (PPLO) (*16*), *Hansenula polymorpha* amine oxidase (HPAO, recently reclassified as *Pichia angusta*) (*17*), and *Arthrobacter globiformis* amine oxidase (AGAO) (*6*). These CuAOs are dimers with monomeric molecular masses ranging from 70 to 90 kDa, with each monomer containing a single active site composed of TPQ and a Cu(II) atom (*18*−*20*). Each monomer has a pair of β-hairpin arms, which extend from one subunit across the face of the other subunit. One of these arms partially defines the entrance to the active site channel in the other subunit. The residues of this arm vary among the CuAOs and may play a role in substrate recognition (*17*). Differences in amino acid composition in this region introduce unique characteristics to a given CuAO in terms of the electrostatic properties and dimensions of the active site channel, as well as the degree of substrate accessibility to TPQ (*16*, *21*).

Copper-containing amine oxidases oxidize primary amines through a ping-pong mechanism (Scheme 1). The key step in catalysis is the conversion of the initial "substrate Schiff base", a quinoneimine, to the "product Schiff base", a quinolaldimine (**B** → **C**). This conversion is facilitated by a conserved aspartate acting as a general base assisting proton abstraction from the alpha carbon of the substrate (*22*, *23*). Subsequently the aldehyde product is released through hydrolysis, yielding Cu(II)-aminoresorcinol in equilibrium with Cu(I)-semiquinone (**D** ↔ **E**). In the presence of O_2, oxidation to an iminoquinone species occurs, producing H_2O_2. This species is then hydrolyzed, liberating NH_4^+ and the resting cofactor (**F** → **A**) (*6*). In addition, NH_4^+ may be released by a transimination reaction between the iminoquinine and substrate, thereby forming the "substrate Schiff base" (**F** → **B**) (*24*). It is possible that there are slight variations among CuAOs with respect to the mechanism for reoxidizing the reduced quinone species. In a proposed alternate mechanism for the reoxidation of TPQ_{red} in HPAO, the reduction of Cu(II) to Cu(I) is not required (*25*−*27*).

Given the imine shift accompanying Cα proton abstraction (Scheme 1, **B** → **C**), mechanism-based inhibitors for CuAOs may be developed by incorporating either a halogen group or unsaturation at the β-position of a potential substrate molecule. Examples are β-bromoethylamine (*28*−*33*) and propargylamine (*30*). The former case results in an S_N2-activated α-haloaldehyde product, whereas the latter case results in an electrophilic α,β-unsaturated aldehyde product. These compounds have been effectively studied as inhibitors of plasma amine oxidase (*30*), SSAO (*34*, *35*), and MAOs (*36*−*38*). In addition, we have successfully used this strategy in designing a set of compounds, which were tested against six CuAOs (*21*). An important finding was that 4-(2-naphthyloxy)-2-butyn-1-amine (**1**) is a particularly effective inhibitor of AGAO. Given this result, we felt that an evaluation of a series of 4-aryloxy analogues of **1** might reveal insight to achieving potent and selective inhibition of the various copper amine oxidases.

In this study, the analogues investigated in addition to **1** were 4-(1-naphthyloxy)-2-butyn-1-amine (**2**), 4-(2-methylphenoxy)-2-butyn-1-amine (**3**), 4-(3-methylphenoxy)-2-butyn-1-amine (**4**), 4-(4-methylphenoxy)-2-butyn-1-amine (**5**), and 4-phenoxy-2-butyn-1-amine (**6**) (Figure 1). These compounds have been screened against PSAO, PPLO, KDAO, AGAO, EPAO (equine plasma amine oxidase), and

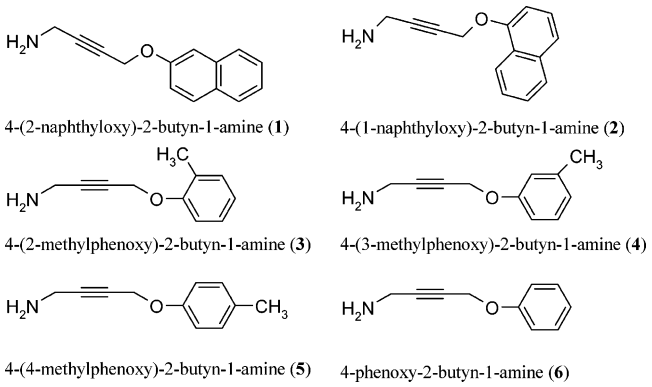

FIGURE 1: Inhibitor compounds.

BPAO (bovine plasma amine oxidase) for potency, reversibility, and selectivity. For comparative purposes, partition ratios and IC_{50}'s were determined. Thorough analysis of the behavior with each compound was performed with AGAO, establishing a baseline for comparison with the other CuAO enzymes studied. In addition, the structures of AGAO complexed with 4-(2-naphthyloxy)-2-butyn-1-amine (**1**) and 4-(4-methylphenoxy)-2-butyn-1-amine (**5**) have been determined. These structures suggest a novel inhibition mechanism for the 4-aryloxy compounds involving covalent modification of the reduced TPQ cofactor. Furthermore, a possible correlation between inhibitor potency and active-site fit is discussed. Collectively, these results help to establish the molecular foundations governing substrate specificity/inhibitor potency for AGAO. Moreover, the results presented herein support the feasibility of designing selective CuAO inhibitors.

MATERIALS AND METHODS

Enzyme Purification and Isolation. PPLO was purified using minor modifications of a published protocol (*39*). A bead beater was used to break the cells, and the use of a Concanavalin A column was eliminated. EPAO was purified according to (*40*). KDAO was purified from Drosophila S2 cells as previously described (*8*). PSAO, BPAO, and AGAO were purified using previously published protocols ((*9*, *41*, *42*), respectively).

Inhibitor Synthesis. The six compounds used in this study, 4-(2-naphthyloxy)-2-butyn-1-amine (**1**), 4-(1-naphthyloxy)-2-butyn-1-amine (**2**), 4-(2-methylphenoxy)-2-butyn-1-amine (**3**), 4-(3-methylphenoxy)-2-butyn-1-amine (**4**), 4-(4-methylphenoxy)-2-butyn-1-amine (**5**), and 4-phenoxy-2-butyn-1-amine (**6**) were synthesized and characterized as previously described (*43*).

Steady-state Kinetics and Absorption Spectra. Kinetic assays and absorption spectra were collected using a Varian Cary 6000i scanning UV/Vis/NIR spectrophotometer equipped with a dual-cell peltier accessory for temperature control. All protein concentrations were based on previously published extinction coefficients at 280 nm: PPLO (*44*), EPAO (*7*), AGAO (*42*), PSAO (*9*), BPAO (*45*), and KDAO (*8*). All spectra were recorded at 25 °C. Stock solutions of inhibitor were prepared by adding the appropriate amounts of doubly deionized water and compound to yield a final concentration near 10 mM. When necessary, 1-mM solutions of inhibitor were prepared by diluting the 10-mM stock with doubly deionized water. Freshly thawed protein stocks were diluted to ~0.5 mg/mL with 0.1 M potassium phosphate buffer, pH 7.2. Whenever possible, the same protein stock was used for all experiments. Benzylamine was used as a control substrate in all experiments except with KDAO, for which 4-(dimethylaminomethyl)benzylamine (DAB) was used (*8*).

Enzyme samples were incubated at 4 °C with varying excesses of inhibitor based on active-site concentration as previously described (*21*). At various times, 30−80-μL aliquots were removed and diluted into a benzylamine assay mixture (3 mL total volume) at 25 °C. Activities were determined at least in triplicate by monitoring the production of benzaldehyde at 250 nm over 3 min using an extinction coefficient of 12 800 $M^{-1}cm^{-1}$ (*29*, *46*), and were reported in spectroscopic units (change in absorbance/min) per mg of protein. Although excess inhibitor was not removed prior to assaying, it was diluted at least 37-fold in the final assay volume. Loss of activity occurred over a short period of time, and had plateaued by 30 min in every case in which a partition ratio was calculated (or the activity reached zero). Partition ratios were calculated from these data by plotting the percent residual activity versus [inhibitor]/[active site]. The error associated with the partition ratio was obtained from the linear fit of this plot using Origin 7.0 software (Microcal, MA). Furthermore, IC_{50} values for 30-min incubations were obtained by plotting plateau activity against the concentration of inhibitor. For KDAO, the above procedure was modified in that protein/inhibitor solutions were incubated at 30 °C, DAB was used as substrate, a 1.5-mL total assay volume was used, and protein/inhibitor solutions were kept at 25 °C between assays.

The ability of the enzymes to use the inhibitors as substrates was measured using a horseradish peroxidase (HRP)-ABTS (2,2′-azino-bis(3-ethyl)-benzthiazoline-6-sulfonic acid) coupled assay. HRP reacts with hydrogen peroxide producing an activated form that in turn oxidizes ABTS to produce a product with a λ_{max} at 414 nm (*21*, *47*). Activities, determined from the ΔA_{414}, are reported in μg product·(min^{-1}·mg^{-1}) of protein (*48*). Substrate concentrations were adjusted to 300 μM in a total assay volume of 2 mL. All assays were performed in 0.1 M potassium phosphate buffer, pH 7.0 at 30 °C.

Phenylhydrazine Titration. To examine the degree of reversibility of inhibition, protein solutions were incubated at 4 °C for 30 min with a sufficient quantity of inhibitor to inactivate the enzyme, as determined via direct assay. Gel filtration chromatography (Sephadex G-25) was used to remove unbound inhibitor from the protein-inhibitor complex. Fractions containing protein were then pooled, concentrated, and their spectra and activities were recorded. The concentrated protein was dialyzed against four 1-L buffer exchanges of 0.1 M potassium phosphate buffer, pH 7.2 over a period of 36 h. Post-dialysis, spectra and activities were again measured, and phenylhydrazine titrations performed. The dialyzed enzyme−inhibitor complexes were titrated with substoichiometric quantities of freshly prepared phenylhydrazine in anaerobic 0.1 M potassium phosphate buffer, pH 7.2 to a maximum of a threefold excess over the protein concentration. Phenylhydrazine reacts with unmodified TPQ by forming a stable adduct (yellow) with a λ_{max} at ~450 nm and an extinction coefficient of 32 000 $M^{-1}cm^{-1}$(*41*). No reaction should be observed if either the inhibitor is co-

valently bound to TPQ or if the inhibitor is bound in a manner that prevents access of phenylhydrazine to TPQ.

To check for possible cofactor modification of PPLO by **5**, a control sample of PPLO and one fully inhibited with compound **5** were diluted with 8 M urea in 0.1 M potassium phosphate buffer, pH 7.2 to a final concentration of ~7 μM. A spectrum was recorded. A 10-fold excess of phenylhydrazine in anaerobic 0.1 M potassium phosphate buffer, pH 7.2 was added, and spectra were taken until no further reaction was observed.

Nitroblue Tetrazolium Assays. Inhibited samples of AGAO (7.4 μM), PPLO (7.8 μM), and BPAO (20 μM) were tested for TPQ redox competency using a nitroblue tetrazolium (NBT) assay as described previously (*21*, *43*). This assay tests the ability of the TPQ cofactor in the denatured preparation (SDS and β-mercaptoethanol (BME)) to mediate O_2-dependent redox cycling oxidation of glycinate. Enzyme samples were incubated with a sufficient quantity of inhibitor to yield at least 97% inactivation, and were then denatured using a standard denaturing buffer (10% SDS with 0.5 M BME). The denatured samples were run in duplicate on a polyacrylamide gel, which was cut in half and stained with either Coomassie blue or NBT in 2 M potassium glycinate.

*Crystals and X-ray Diffraction Data for an AGAO − 4-(2-naphthyloxy)-2-butyn-1-amine (**1**) Complex*. Crystals of the complex were grown using the vapor diffusion method in hanging drops. A solution of AGAO (10 mg/mL in 50-mM HEPES, pH 7.0) was incubated with a fivefold molar excess of compound **1** for 4 h at room temperature. Hanging drops were comprised of 4 μL of the protein-inhibitor mixture added to an equal volume of the well solution (1.5 M $(NH_4)_2SO_4$, 260 μM $CuSO_4$, 100 mM MES, pH 6.5). Crystals grew after several weeks at 20 °C. Prior to recording diffraction data, the crystals were cryoprotected by successive transfers through well solutions containing increasing amounts of glycerol (2.5% increments) to a final concentration of 30% over a period of 2 h. The glycerol-doped well solutions also contained 2.5 mM EGTA to remove excess copper from the buffer.

X-ray diffraction data were recorded at the Stanford Synchrotron Radiation Laboratory Beamline 7−1 at a wavelength of 1.08 Å from a crystal flash-frozen in a stream of nitrogen gas at 100 K. The images were recorded on a Mar345 imaging plate detector. The diffraction data were integrated and scaled using programs DENZO and SCALEPACK (*49*).

*Crystals and X-ray Diffraction Data for an AGAO−4-(4-methylphenoxy)-2-butyn-1-amine (**5**) Complex*. Crystals of AGAO were grown using the hanging-drop vapor diffusion method. Hanging drops were comprised of 2 μL of protein solution (10 mg/mL in 50 mM HEPES, pH 7.0) mixed with an equal volume of well solution (1.1 M $(NH_4)_2SO_4$, 150 mM sodium citrate, pH 6.5). Crystals grew during several weeks at 20 °C. The protein-inhibitor complex was prepared by soaking crystals in compound **5** during the cryoprotection procedure, which was similar to that described for the AGAO-compound **1** complex. However, in this case all glycerol-doped well solutions contained a tenfold molar excess of compound **5**, but lacked the addition of EGTA since these crystals were grown in the absence of additional copper. The crystals were left in the 20% glycerol cryoprotectant (with compound **5**) for 48 h and then transferred to a 30% glycerol solution over the 30 min prior to flash freezing.

Data were recorded on a laboratory X-ray source comprising a Rigaku RU-200 rotating anode generator with Osmic mirror optics and a copper anode (wavelength 1.5418 Å) with the crystal maintained at 100 K in a stream of nitrogen gas. The images were recorded on a Mar345 imaging plate detector. The X-ray diffraction data were integrated and scaled using the programs MOSFLM (*50*) and SCALA (*51*).

Crystal Structure Refinement. The starting model for the refinement of each of the complexes was the structure of native AGAO refined at 1.6 Å resolution (D. B. Langley, H. C. Freeman, J. M. Guss, unpublished results). The water molecules, metal ions, sulfate ions, and glycerol were removed from the starting model and the TPQ was modeled as an Ala residue. The refinements proceeded in the following steps: rigid body refinement at low resolution (3.5 Å); restrained refinement using REFMAC5 (*52*) with automatic selection of solvent molecules using ARP/WARP (*53*), removal of any water molecules in the active site channel, examination of electron-density difference maps using program O (*54*), addition of the active-site copper atom, manual adjustment of several residues in the active site channel, additional restrained refinement with individual atomic thermal parameters, examination of electron-density difference maps, and addition of sulfate ions and glycerol molecules. The entire structure and all solvent molecules were manually checked for position, sensible geometry, and chemical interactions including hydrogen-bond formation in respective electron-density maps**.** At this stage, the most significant remaining ($F_{obs} - F_{calc}$) electron-density in both structures were in the active sites (Figure 3). The electron-density was consistent with the presence of bound inhibitors, which were constructed using PRODRG (*55*) and the CCP4 molecular library sketcher (*51*), included in the model and refined. The restraint library used for the inhibitors included bond lengths, bond angles and planarity, but not torsion angle restraints. The structures were validated with MOLPROBITY (*56*) and PROCHECK (*57*). A summary of the X-ray data collection and refinement is presented in Table 4. The entire experiment and refinement were repeated using a crystal of AGAO and **1** obtained by soaking rather than cocrystallization. The outcome was identical. The coordinates and structure factors for the complexes of AGAO with compounds **1** and **5** have been deposited with the Protein Data Bank as entries 1SII and 1SIH, respectively.

RESULTS

General Compound Effectiveness. To investigate the overall potency of inhibition, concentration-dependent data were obtained by the aforementioned methods (Table 1). The data represent only two inhibitor concentrations for each enzyme−inhibitor couple, and do not show all of the data obtained for the determination of partition ratios and IC_{50} values reported in Table 2. Based on the data in Tables 1 and 2, the following trends in relation to inhibitor potency are observed: (a) compound **2**: AGAO > PPLO > BPAO > EPAO > KDAO > PSAO; (b) compound **3**: AGAO > PPLO > BPAO > EPAO ≈ PSAO > KDAO; (c) compound

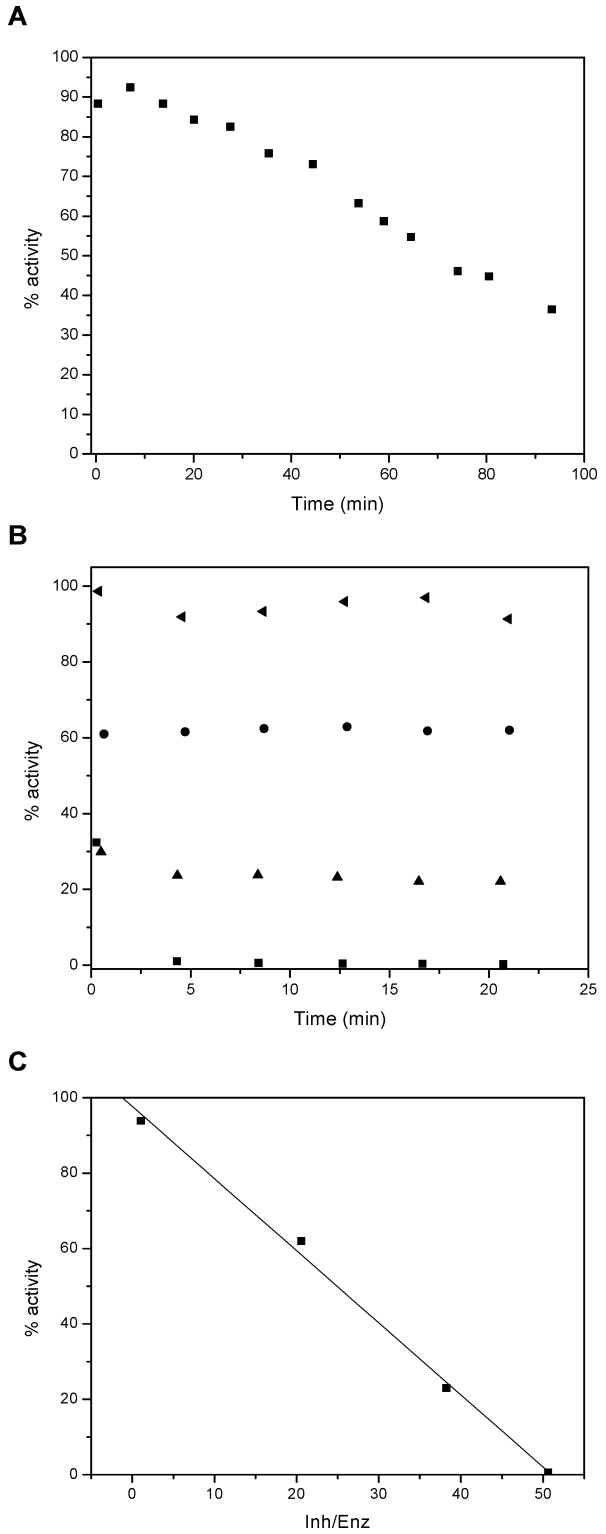

FIGURE 2: Typical data plots for inhibited CAOs. Panel (A) Classic time-dependent inactivation of EPAO (~4.6 μM active site concentration) by 427-μM compound **3**. (B) Activity for PPLO (3.82 μM active site concentration) with varying amounts of compound **6** over time: 4 μM (left facing solid triangles), 79 μM (●), 146 μM (▲), 193 μM (■). See Materials and Methods for experimental procedure. (C) Partition ratio plot for PPLO with compound **6**.

4: AGAO > PPLO; (d) compound **5**: AGAO ≈ BPAO > PPLO > EPAO ≈ KDAO ≫ PSAO; (e) compound **6**: AGAO ≫ PPLO > BPAO > KDAO > PSAO > EPAO; (f) potency of compounds in inactivating AGAO: **1** > **2** > **4** ≈ **5** ≈ **6** > **3**.

Although some inhibitor-enzyme combinations resulted in time-dependent loss of activity over the period of several minutes to 1 h, for example EPAO (see Figure 2, panel A), in the majority of cases examined for compounds **2**−**6**, this time-dependent loss of activity was found to occur within the first ~30 s following addition of inhibitor, with the subsequent residual activity remaining constant (Figure 2, panel B). As the concentration of inhibitor was increased, the initial drop in activity was greater. This behavior indicates a classical partitioning between turnover and inactivation, with the constant residual activity signaling complete metabolism of the inhibitor. From the plots of residual enzyme activity versus the ratio of inhibitor concentration to active site concentration, partition ratios were calculated (Figure 2, panel C) (*58*). In certain cases (such as PSAO with compound **2** and EPAO with compound **6**), the decrease in residual enzyme activity achieved upon increasing concentrations of inhibitor reached the same plateau activity so that complete inhibition was never achieved, and partition ratios were not determined. This behavior is typical of product protection, suggesting that the turnover aldehyde product protects the enzyme against further inactivation. In cases where the observation of high partition ratios indicated substantial normal substrate turnover, we expected to find good substrate activity when this was measured directly, and this was borne out by data listed in Table 3. Indeed, the 4-aryloxy compounds were discovered to be oxidized at varying but substantial rates relative to benzylamine.

To investigate the degree of reversibility of inhibition, phenylhydrazine titrations were performed on selected inhibited samples (see Materials and Methods). In the cases tested (see Table 2, compounds **2** and **3**), only BPAO displayed reactivity with phenylhydrazine, though this was relatively low (~13% and 22%, respectively), suggesting that phenylhydrazine may displace the bound inhibitors to a limited degree. Additionally, samples of PPLO, BPAO, and AGAO that were at least 98% inhibited by compound **5** were denatured and examined for redox integrity of the TPQ cofactor through the redox cycling NBT assay. In the cases of BPAO and AGAO, the redox activity was indistinguishable from the control activity (data not shown), indicating either that inactivation arises from covalent modification of an active site or channel residue that blocks access of the substrate, or from covalent modification of the cofactor in a manner that is reversible upon enzyme denaturation. In the case of PPLO, no reaction with NBT was observed for either the control enzyme or the inhibited sample, suggesting that denaturing of PPLO with SDS/BME might modify the TPQ cofactor. Therefore, to test reversibility of the modified TPQ adduct in PPLO, samples were denatured with 8 M urea and titrated with phenylhydrazine. While the control PPLO sample reacted quite rapidly with phenylhydrazine to a final extent of 9.7 μM TPQ (1.5 TPQ/dimer), the inhibited sample reacted much more slowly. Over a period of 17 h, 3.4 μM TPQ (0.5 TPQ/dimer) was found to react with phenylhydrazine (data not shown), indicative of at least some reversibility of cofactor modification.

Deviation from Trends in Reactivity. While general trends in reactivity were consistent among all CuAOs tested, a few notable deviations were observed. AGAO displayed interesting behavior with compound **6** in that there was an initial drop in activity within 30 s followed by a slow decrease in

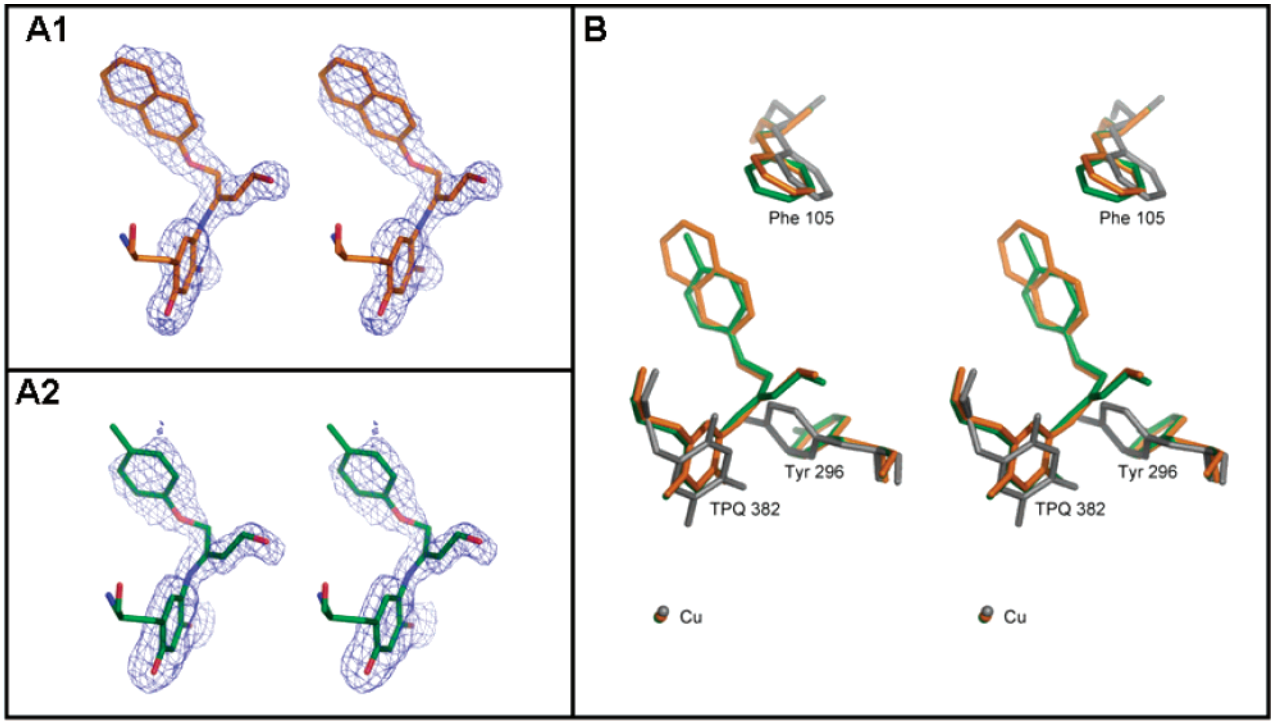

FIGURE 3: Electron density and stereo overlay of the TPQ/inhibitor moieties. (A1) Stereoview of the TPQ_{amr}-4-(2-naphthyloxy)-2-butenal moiety. (A2) Stereoview of the TPQ_{amr}-4-(4-methylphenoxy)-2-butenal moiety. Both structures have been solved to 1.7 Å resolution. (B) Stereoview of the overlayed structures of native AGAO (grey), TPQ_{amr}-4-(2-naphthyloxy)-2-butenal moiety (orange), and TPQ_{amr}-4-(4-methylphenoxy)-2-butenal moiety (green).

Table 1: Inhibition of Select Amine Oxidases by Compounds in Figure 1

enzyme[c]	compound	excess inhibitor[a]	% activity[b]	enzyme[c]	compound	excess inhibitor[a]	% activity[b]
AGAO	2	stoich	53	AGAO	5	stoich	94
		5	2			10	25
PPLO	2	stoich	89	PPLO	5	stoich	92
		25	0			30	0
EPAO	2	stoich	95	EPAO	5	stoich	86
		72	51			29	17
PSAO	2	102	80[d]	PSAO	5	stoich	93
BPAO	2	stoich	88			30	90
		52	6	BPAO	5	stoich	65
KDAO	2	stoich	83			30	2
		60	73	KDAO	5	stoich	29
						30	30
AGAO	3	stoich	98	AGAO	6	stoich	98
		31	2			13	0
PPLO	3	stoich	87	PPLO	6	stoich	94
		61	0			51	0
EPAO	3	92	38[d]	EPAO	6	101	59[d]
PSAO	3	stoich	92	PSAO	6	96	43[d]
		102	20	BPAO	6	stoich	96
BPAO	3	stoich	89			97	17
		78	23	KDAO	6	stoich	98
KDAO	3	stoich	83			30	79
		28	80				
AGAO	4	stoich	95				
		10	29				
PPLO	4	stoich	92				
		30	16				

[a] Excess inhibitor relative to active site concentration. "Stoich" indicates concentration of inhibitor is equal to that of the active site. [b] Activity remaining relative to uninhibited enzyme after activity plateaued. Numbers are average of at least three assays (rounded to nearest integer). [c] Active site concentrations: AGAO, 5.7−7.1 μM; PPLO, 3.1−4.8 μM; EPAO, 3.6−5.2 μM; PSAO, 5.3−7.3 μM; BPAO, 2.9−9.2 μM; KDAO, 4.3−5.6 μM. [d] In these cases, classical time-dependent inactivation is observed.

activity until a plateau was reached after about 30 min, whereas the activity of all other compounds tested with AGAO remained constant once the initial drop in activity within the first 30 s of the assay had occurred. This unique behavior prompted additional experiments to examine the possibility of a biphasic reaction mechanism. Identical samples of AGAO were incubated with a 20-fold excess of inhibitor. The first sample was subjected to gel filtration and dialyzed against 0.1 M potassium phosphate buffer, pH 7.2 following a 30 min incubation with compound **6** (resulting

Table 2: Potency of Inhibition toward Select Amine Oxidases for the Compounds in Figure 1

enzyme	inhibitor	IC_{50} (μM)	partition ratio
AGAO[a]	2	7	1[b,c]
BPAO[a]	2	148	35 ± 2
EPAO	2	170	84 ± 8
PPLO[a]	2	39	23 ± 2
AGAO[a]	3	97	28 ± 5
BPAO[a]	3	358	80 ± 26
EPAO	3	302	125 ± 20
PPLO[a]	3	118	61 ± 7
PSAO[a]	3	455	125 ± 26
AGAO	4	47	12 ± 2[c]
PPLO	4	91	37 ± 6[c]
AGAO	5	48	12 ± 1[c]
BPAO[d]	5	10	11 ± 2
EPAO	5	83	36[b]
PPLO	5	57	24 ± 1[c]
AGAO[a]	6	50	12 ± 1
BPAO[d]	6	348	107 ± 21[c]
KDAO	6	381	153[b]
PPLO[a]	6	100	51 ± 5[c]

[a] In cases indicated a phenylhydrazine titration of the fully inhibited protein was performed. [b] Based on incomplete data (data fit for only two concentrations of inhibitor). [c] Values determined from plateau activity following 30-min incubation except where noted. In these cases, partition ratios were calculated from the plateau activity observed between 0 and 30 min. [d] For BPAO, phenylhydrazine result presented in ref *43*.

Table 3: Compound Turnover by CuAOs[a,b]

enzyme	benzylamine rate	2[c]	3	4	5	6
EPAO	1	0.28	0.37	ND	0.28	0.34
BPAO	1	4.7	10	ND	4.4	0.81
PPLO	1	0.91	0.87	ND	ND	1
AGAO	1	0	0.72	0.45	0.74	0.54
PSAO	1	2.6	1.9	ND	2.2	2.4

[a] Protein concentration ~ 0.3 μM. [b] Substrate concentration 300 μM. [c] Rates normalized based on the rate of benzylamine oxidation, reported as μmoles product per minute per mg of protein.

in 0% activity remaining). The second sample was treated with compound **6** for 30 s and then immediately subjected to gel filtration to remove excess inhibitor prior to dialysis (resulting in 50% activity remaining). Each sample was then titrated with phenylhydrazine. The first sample showed no detectable reaction with phenylhydrazine, whereas titration of the second sample resulted in ~50% reactivity with TPQ, as expected. This result supports a biphasic reaction mechanism for the inactivation of AGAO by **6**, though there is no evidence for two different inactivation products. Although the nature of the biphasic inactivation of AGAO by **6** remains undefined, one possibility is that it represents an example of the well documented but cryptically elusive case of half-site reactivity (*59*, *60*).

Unlike other amine oxidases with compound **2**, PSAO displayed time-dependent inhibition with this compound (100-fold excess). Activity was reduced to 82% after 30 min and slowly declined thereafter. This fact together with the time-dependent data suggests that compound **2** is an excellent substrate, as well as an inactivator for PSAO, with inhibition occurring infrequently. These results agree well with the behavior described in our previous report for PSAO and compound **1**. PSAO also displayed a slow time-dependence of inactivation with compound **6** (~ 40% activity remaining after 2 h at a 96-fold excess).

EPAO displayed interesting behavior with compound **3** in that time-dependent inactivation was observed at 60- and 90-fold excesses, but no time-dependence was observed at a 30-fold excess or lower. At a 90-fold excess of inhibitor, EPAO activity was ~ 88% of the control after 30 s and 38% after 1.5 h. EPAO also displayed a slow time-dependence of inactivation with compound **6** (59% activity remaining after 1.25 h). Inhibition of PPLO with **6** required between 0.5 and 5 min for the plateau in activity to be reached, whereas the plateau was found to be immediate with all other compounds tested against this enzyme.

Structures of the AGAO-inhibitor complexes. Residual $F_{obs} - F_{calc}$ electron-density differences observed during the refinement of the AGAO complexes of compounds **1** and **5** was interpreted in terms of the inhibitors being bound in the active sites (Figure 3). The orientation of the inhibitors was deduced from the distinctive electron-density corresponding to the naphthyloxy- and methylphenoxy-groups of compounds **1** and **5**, respectively. The TPQ cofactor was linked covalently to an atom of each inhibitor. The new bond joined what was originally the O5 atom of the TPQ to the third carbon along the chain from the original amine group of the inhibitor (Figure 1). Subsequently, the atom types of the linking atom and the terminal atom of the inhibitor were changed to nitrogen and oxygen, respectively, to be consistent with the proposed mechanism of inhibition (see below). In both complexes, the TPQ cofactors are in the "off"-copper conformation. In both cases, the "gate" Tyr296 is in the "open" conformation (Figure 4). The naphthyloxy- and methylphenoxy-groups have identical orientations with respect to the protein and the two inhibitors bind in an almost identical fashion (Figure 4). If the structures of the two complexes are superimposed, the chemically equivalent atoms of the inhibitors and the TPQ cofactors have a root-mean-square difference of 0.32 Å (Figure 3, panel B). The terminal amino (aldehyde) groups of the inhibitors make a short contact (~2.5 Å) with one of the carboxyl oxygen atoms of the catalytic base, Asp298. If the inhibitors have been converted to the equivalent aldehyde, as we propose below, then the close contact is consistent with a hydrogen bond. In this case, the carboxyl group of Asp298 must be protonated.

The AGAO inhibitor structures can be compared with various native AGAO structures. The structures of native and inactivated AGAO are nearly identical with the exception of differences at the active site. It should be noted that different native structures themselves show variation at the active site, particularly with respect to the conformation of the TPQ (which can be modeled as "on"- or "off"-copper) and the nearby "gate" Tyr296 (whose "open" or "closed" conformations govern active-site accessibility to substrate). The high resolution (1.6 Å) (D. B. Langley, H. C. Freeman, and J. M. Guss, unpublished results) structure used as the starting model for these protein complexes has a disordered TPQ and the gate tyrosine in the "closed" conformation**.** In contrast, PDB entries 1AV4 and 1AVL (*6*) have off- and on-copper TPQs, respectively. While in both cases the gate tyrosine is disordered, whereas PDB entries 1IVW and 1IVX (*61*) have on- and off-copper TPQs, respectively; both are modeled with closed gate tyrosine conformations. Variations in the position of TPQ and the gate are the only significant differences among the various native AGAO structures. In

Table 4: Crystallographic Data and Structure Refinement Statistics for *Arthrobacter globiformis* Amine Oxidase

structure	AGAO-**1**	AGAO-**5**
space group	*C*2	C2
unit cell dimensions	$a = 158.06$	$a = 157.65$
	$b = 62.62$	$b = 62.79$
	$c = 91.99$	$c = 91.66$
	$\beta = 112.1°$	$\beta = 112.2°$
resolution (Å)	1.70−19.9 (1.70-1.74)	1.73−22.8 (1.73-1.77)
redundancy	∼10	5−6
R_{merge} [b]	0.034 (0.31)[a]	0.031 (0.20)
I/σ(I)	13 (2.3)	29 (7.4)
completeness (%)	92.7 (76.4)	92.3 (71.2)
non-H atoms refined	5428	5368
no. reflections (working set)	81 489 (5635)	76 191 (4700)
no. reflections (free set)	4333 (323)	4013 (243)
R_{work}	0.157	0.149
R_{free} (5% of data)	0.183	0.168
R_{total}	0.159	0.150
rmsd bond lengths (Å)	0.010	0.010
rmsd bond angles (°)	1.35	1.37
average *B* values (Å^2)	22.7	23.2

[a] Numbers in parentheses refer to the highest (20th) resolution shell. [b] $R_{merge} = \Sigma|I_h - \langle I_h\rangle|/\Sigma\langle I_h\rangle$. [c] *R* values $= \Sigma|F_{obs} - F_{calc}|/\Sigma F_{obs}$. R_{total} is the *R* value following the final cycles of refinement, in which all the data were used.

the structures of the complexes of AGAO with compounds **1** and **5**, presented in this work, it is sterically necessary that the TPQ residues are off-copper and the gate tyrosines are in the open conformation.

Other more subtle movements with respect to the native structures have occurred, being required to accommodate each of the covalently linked inhibitors. The position of Phe105, which lines the active site channel, differs by a movement of the C^{α} (∼1 Å) and by a rotation of its side chain (70° about the $C^{\beta}-C^{\gamma}$ bond) to interact with the naphthyloxy- and methylphenoxy-groups of the inhibitors (Figure 4). The polypeptide backbone on either side of Phe105 (Leu100 through Val108) moves as a consequence. The side chain of Glu106, which is disordered in the unpublished 1.6 Å native structure as evidenced by the absence of electron density, is well resolved in both inhibitor complexes. Pro136, which is close to Phe105, moves ∼1.0 Å (C^{γ}) to form a hydrogen bond from its peptide oxygen atom to the hydroxyl oxygen atom of Tyr302. The −OH group of Tyr302 also moves ∼1 Å to form this new hydrogen bond. In the native structure, the peptide oxygen atom of Pro136 forms a hydrogen bond to a water molecule in the substrate access channel. Leu137 also moves ($C^{\delta 2}$ ∼0.9 Å) thus avoiding a steric clash with the gate tyrosine (Tyr296) and the inhibitors. The side chain of Ile379 moves slightly ($C^{\gamma 2}$ ∼1.3 Å) to a position where it is able to maintain hydrophobic packing with Tyr302, as well as to allow space for the product aldehyde ends of each inhibitor.

Residues comprising the hydrophobic cleft, which accommodates the hydrophobic naphthyloxy and methylphenoxy moieties, can be classified according to their approximate position with respect to the common plane of the aromatic rings. Gly380, Ile379, and Trp168 lie on the "TPQ-side" of this ring plane and Ala135, Pro136, Leu137, and Tyr296 lie on the other side. Tyr302 and Phe407 lie on the edges of the aromatic rings (Figure 4). Phe105, and two hydrophobic residues Leu358 and Trp539 (from the β-arm of the adjacent subunit), lie at the end of the channel near the inhibitors. The positions of the residues on the β-arms of the native and complex structures are identical within the limits of precision.

DISCUSSION

The most common design of CuAO mechanism-based inhibitors has incorporated unsaturation at the β-position of the substrate amine (*43*, *62*, *63*). For simple propargylic or haloallylic amines, turnover results in an electrophilic α,β-unsaturated aldehyde product, which can bind covalently at the active site (to TPQ or an active site residue). In some cases, metabolism of the suicide substrate results in channeling directly to a modified cofactor incapable of reoxidation (*64*). Evidence for covalent modification of active-site residues by an electrophilic turnover product has been presented by Frebort et al., who studied the inhibition of *Aspergillus niger* amine oxidase (*65*) and grass pea amine oxidase (*66*) by 1,4-diamino-2-butyne. An additional example where inhibition can result from covalent modification of channel residues is the inactivation of AGAO by a lysine-directed chemical modification agent (*67*).

Relevant for understanding and interpreting the data presented herein are the inhibitory effects of 4-(2-naphthyloxy)-2-butyn-1-amine (**1**) with AGAO and PSAO as reported by Shepard et al (*21*). Compound **1** was found to inactivate AGAO completely at stoichiometric concentrations. In addition, no oxidation of **1** by AGAO could be detected. Despite the fact that AGAO fully inhibited by **1** showed no reactivity toward phenylhydrazine, NBT staining of fully inactivated enzyme was indistinguishable from the control enzyme preparation, indicating that the TPQ-inhibitor adduct formed was reversible under denaturing conditions. In contrast to AGAO, PSAO activity was virtually unaffected even by a large excess of compound **1**, and **1** was subsequently discovered to be an excellent substrate. This was consistent with computer modeling results that showed that the active site channel of PSAO could accommodate **1** without any unfavorable nonbonding interactions (*21*). In the case of the AGAO-**1** complex, computer modeling provided no indication of a specific mode of inhibition, though several residues comprising a hydrophobic pocket in AGAO were identified that could potentially interact with the naphthyl group of the inhibitor.

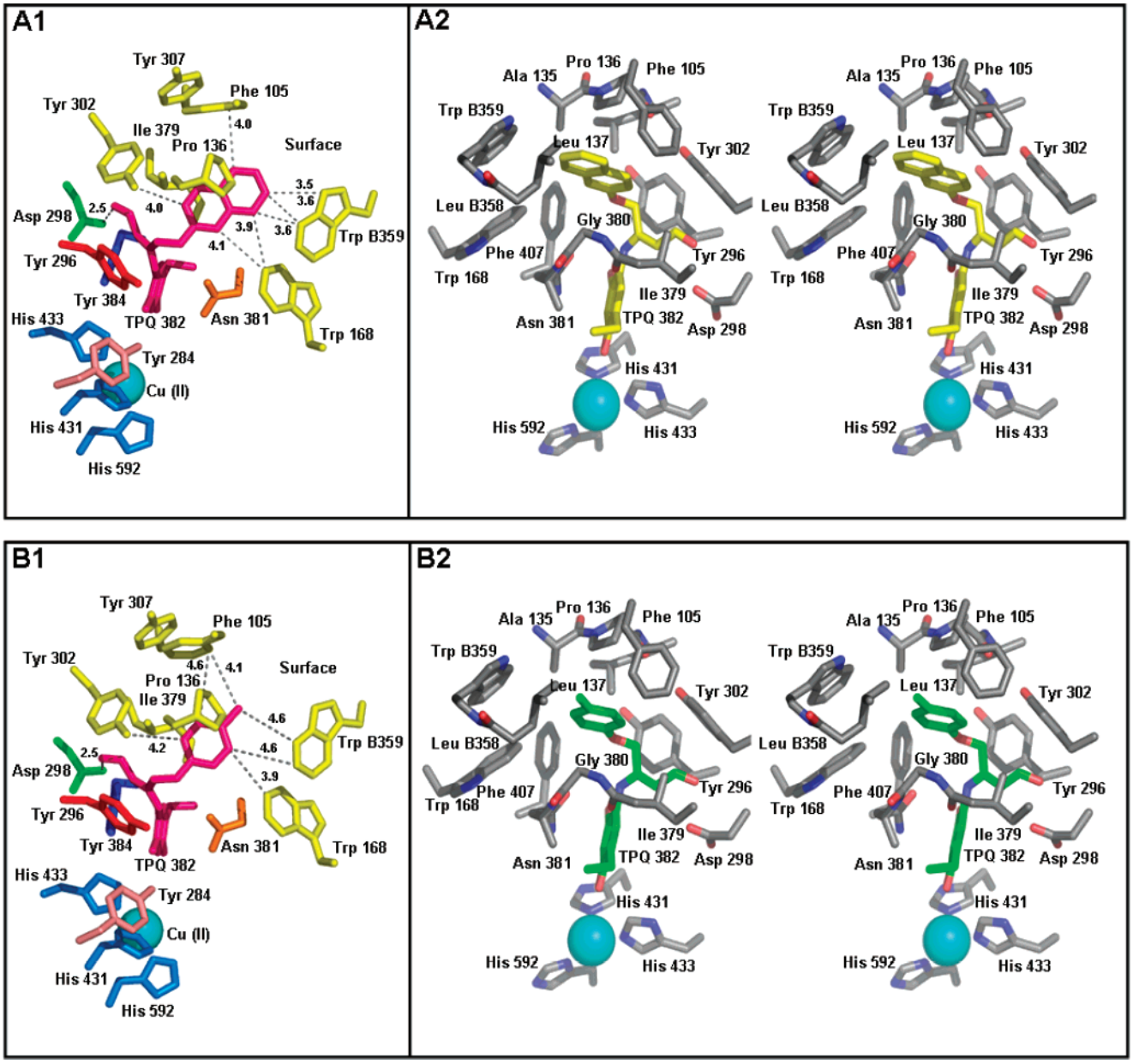

FIGURE 4: TPQ derivatized with two 4-(aryloxy)-2-butynamines. (A1) TPQ_{amr}-4-(2-naphthyloxy)-2-butenal moiety positioned in the active site of AGAO. (A2) Stereoview of the active site of the AGAO-TPQ_{amr}-4-(2-naphthyloxy)-2-butenal structure. (B1) TPQ_{amr}-4-(4-methylphenoxy)-2-butenal moiety positioned in the active site of AGAO. (B2) Stereoview of the active site of the AGAO-TPQ_{amr}-4-(4-methylphenoxy)-2-butenal structure. Views shown in panels A2 and B2 are oriented differently then the views shown in A1 and B1. In panels A1 and B1, the residues composing the hydrophobic pocket are colored yellow and the TPQ/inhibitor moiety is magenta. Distances shown are from residues in the hydrophobic pocket to each respective substituent group of the 4-(aryloxy)-2-butenal moieties. In panels A1 and B1, "surface" indicates the interface between bulk solvent and the protein-derived substrate channel (see Figure 5). In panels A2 and B2, residues are colored by atom (grey, carbon; blue, nitrogen; red, oxygen) with the exception of the TPQ/inhibitor moieties in which carbon atoms are colored yellow and green, respectively. "B" indicates that the residue is derived from the β-arm of the other monomer.

In the current study, we explored the ability of a series of 4-(aryloxy)-2-butyn-1-amine analogues (**2**−**6**) of **1** to inhibit AGAO, PSAO, and four other CuAO enzymes. The α-naphthyl isomer **2** was about half as potent against AGAO as the β-naphthyl isomer **1** (Tables 1 and 2). As in the case of compound **1**, no detectable oxidation of compound **2** by AGAO was observed. The *ortho*- (compound **3**), *meta*- (compound **4**), and *para*- (compound **5**) methylphenoxy analogues and the unsubstituted phenoxy compound **6** were all at least 10 times less effective than compound **2** toward AGAO. However, **4**, **5**, and **6** were considerably more potent than **3**.

When examining the overall potency trends displayed by all six compounds with each CuAO evaluated, it is interesting to note that no single trend holds for all the enzymes. In the cases of AGAO, BPAO, and PPLO, compound **1** was the most effective inhibitor (*21*). In the case of PSAO, **1** and **2** acted as excellent substrates. Compound **5** was the most effective inhibitor of both EPAO and KDAO, and in both cases was at least twice as effective as the other compounds screened. Compound **6** was the least effective inhibitor of BPAO and EPAO, but was more efficient against KDAO than either **1**, **2**, or **3**. In no instance was inhibition found to be reversible through dialysis, but BPAO inhibited with

Scheme 2: Proposed Mechanism of Inhibition for 4-(2-naphthyloxy)-2-butyn-1-amine (**1**) and Related Compounds

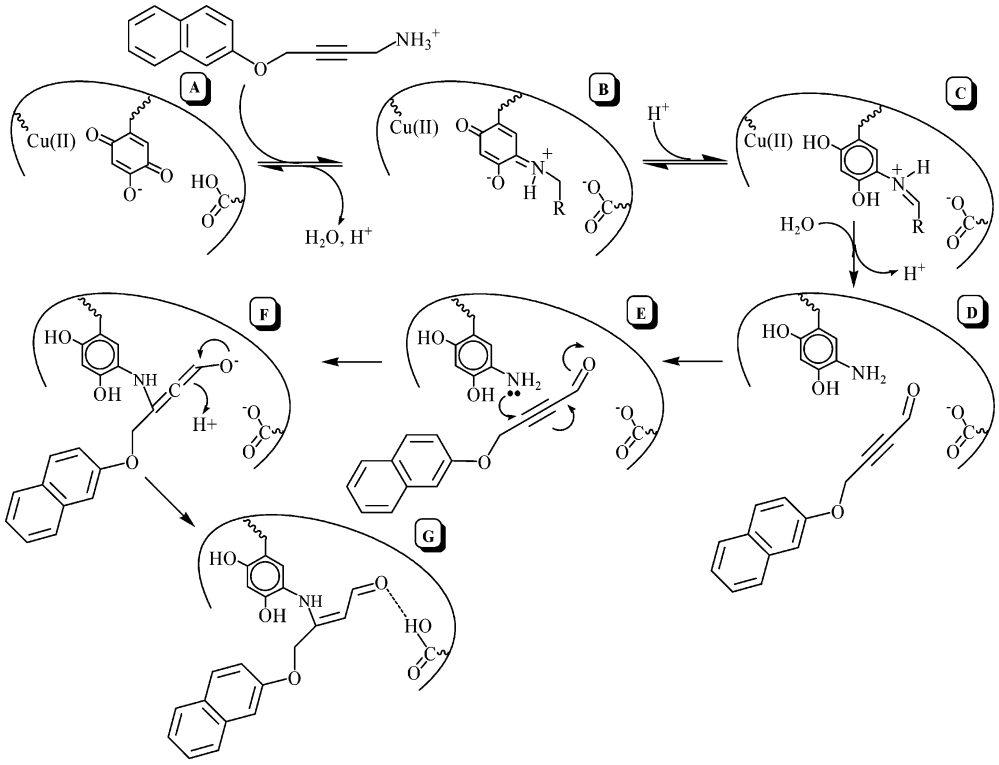

compounds **2** and **3** exhibited slight phenylhydrazine reactivity. In addition, the redox integrity of the TPQ was found to be restored with inhibited samples of BPAO, AGAO, and PPLO upon denaturation (see below).

To gain an insight into the structural basis of the inactivation of AGAO by this class of inhibitors**,** crystal structures of AGAO derivatized by compounds **1** and **5** were refined at high resolution (Figures 3 and 4). These structures identify a novel and completely unexpected modification of the TPQ cofactor. From the bent geometry of the electron density corresponding to the TPQ-inhibitor moiety (Figure 3) it is clear that the TPQ is covalently attached to the middle position of the inhibitor. Although the carbon−carbon triple bond in the reactants **1** and **5** (Figure 1) is unreactive, the observed electron density is consistent with an adduct that would result from nucleophilic attack by the amino group of the reduced aminoresorcinol cofactor (TPQ_{amr}) at C3 of the propargyl aldehyde turnover products of **1** and **5** (Scheme 2). The naphthyloxy and methylphenoxy groups of **1** and **5** are indeed similarly positioned within the hydrophobic binding pocket suggested previously (*21*) (Figures 3 and 4). Comparing the AGAO-**1** and AGAO-**5** structures shows that there is no significant shift of any active-site residue.

A reaction mechanism that accommodates these findings is shown in Scheme 2. The initial steps in the catalysis of the inhibitor are the same as for a normal amine substrate. First, the "substrate Schiff base" is converted to the "product Schiff base" (**B** → **C**) facilitated by a conserved aspartate acting as a general base and abstracting a proton from the α carbon of the inhibitor. Following hydrolysis of the "product Schiff base", the highly electrophilic (at C3) α,*β*-unsaturated aldehyde is released into the active site. Subsequently, nucleophilic attack by the amino group of TPQ_{amr} at the C3 position (**E** → **F**) completed by proton transfer to C2 (**F** → **G**) results in formation of the final TPQ_{amr}-4-(aryloxy)-2-butenal derivatives observed in the respective crystal structures (Figures 3 and 4). Although the observed electron density would also be consistent with adduction of the α,*β*-unsaturated aldehyde turnover product to the triol form of the reduced cofactor rather than TPQ_{amr} (we cannot distinguish −O− from −NH−), it is not clear what scenario would lead to such an alternative adduct.

To permit the C3 of the product aldehyde to get within a reasonable distance for reaction with TPQ, some active-site rearrangement must occur. This might simply involve the aldehyde product moving ∼3.5 Å down the channel until the nucleophile and its target are in suitable proximity (Figure 5). Whatever the mechanism, it is particularly efficient for compound **1**, for which the product of every turnover event then forms an inactivation event adduct.

Given the relationship of each 4-(aryloxy)-2-butenal compound to the hydrophobic pocket in AGAO (Figure 4, panels A and B), it is plausible that the extent of van der Waals interactions between pocket and inhibitor may be the main determinant of potency. The inhibitors that contain the largest substituents (**1** and **2**) are also the most potent against AGAO. Compared with the phenoxy and methylphenoxy substituents, the naphthyloxy group makes more extensive van der Waals interactions with the hydrophobic pocket. The two-fold weakening of the α-naphthyloxy relative to *β*-naphthyloxy inhibitor might simply reflect a better steric fit of the more linearly extended *β*-naphthyl substituent (Figure 1). This suggests that the interactions of the substituent group with residues in the active site channel, namely those in the hydrophobic binding pocket, may play a key role in determining overall potency of inhibition for AGAO by a wide range of structurally diverse inhibitors.

While the phenoxy- and methylphenoxy- analogues (compounds **3**−**6**) were not stoichiometric in their potency, they displayed decreasing potency in the order **4** ∼ **5** ∼ **6** > **3**.

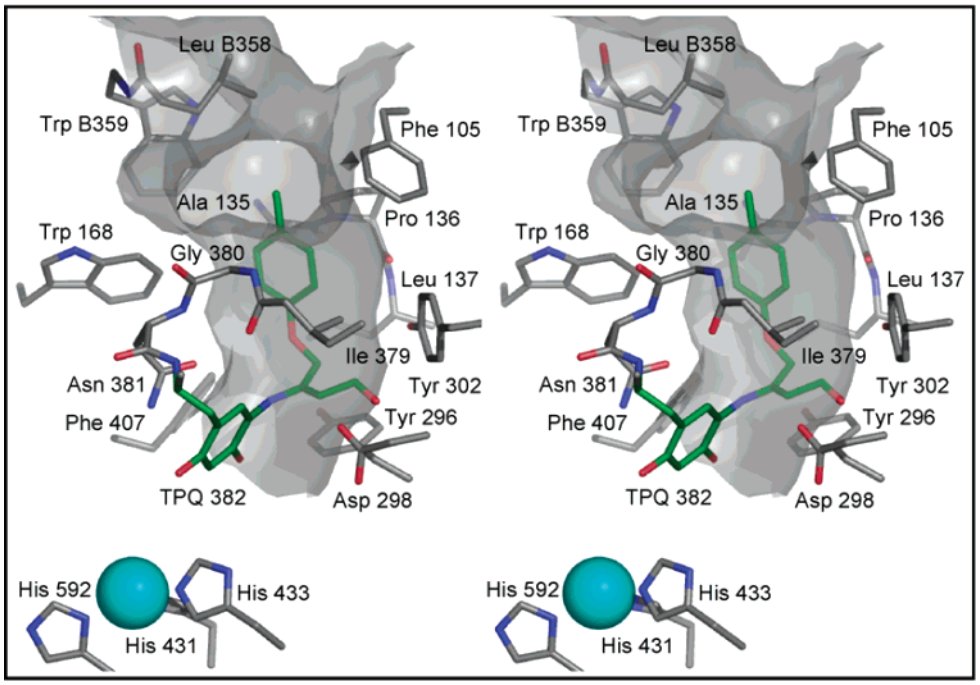

FIGURE 5: Stereoview of the active site channel. Stereoview of the active site channel in the AGAO-TPQ$_{amr}$-4-(methylphenoxy)-2-butenal structure. Atoms are colored as described in Figure 4. The active site channel is shown in gray.

Scheme 3: Proposed Mechanisms for Recovery of TPQ Redox Integrity

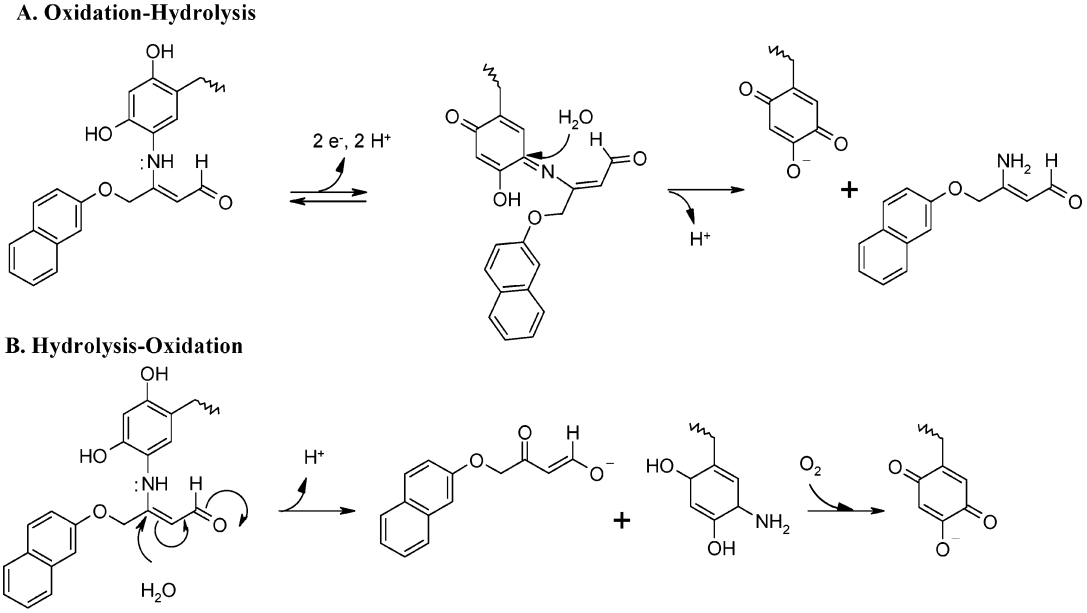

Presumably, the product aldehydes can diffuse from the active site with varying degrees of success. The greater potency of the unsubstituted phenoxy and the *meta*- and *para*-methylphenoxy analogues with respect to the *ortho*-methylphenoxy (**3**) compound suggests that a more or less linearly extended methyl substituent group can project into the hydrophobic pocket in AGAO in a manner that makes more favorable van der Waals contacts for the phenoxy family of inhibitors. Yet, when comparing **3** to **2**, it appears that the phenyl ring interacts more favorably with residues in the hydrophobic pocket (Trp168 and Trp359) than does the *ortho*-methyl substituent.

In terms of the other structurally characterized amine oxidases, a similar hydrophobic pocket was not identified in the modeling studies of **1** with PSAO (*21*). This may explain why the 4-(aryloxy)-2-butynamine inhibitors induce only infrequent inhibition of PSAO. PSAO inhibition is proposed to arise by turnover-product aldehyde modification of surface-exposed Lys residues, obstructing access of the substrate to the active site (*21*, *66*). Likewise, no such hydrophobic binding pocket exists in PPLO, as the channel in this enzyme is extremely open (*16*) and any substrate analogue from this family of compounds interacting with TPQ is likely to be in contact with solvent, as opposed to any residues in the active site channel. However, the lack of a hydrophobic binding pocket in PPLO does not explain the effectiveness of these compounds toward this enzyme in terms of the relatively low partition ratios and IC_{50} values observed (Table 2).

Along these lines, interactions between respective enzymes and inhibitors may not be explained solely by contacts within the active site channel. Despite the observations that for AGAO there exists a likely correlation between an inhibitor's capacity to fill the hydrophobic pocket and its potency, it is clear that these same distinctions do not apply to other CuAOs. As observed in the cases of two amine oxidases lacking this hydrophobic binding pocket, PSAO and PPLO behave very differently when treated with 4-(aryloxy)-2-butynamines. The relatively potent inhibition of PPLO may actually arise as a *direct result* of its relatively solvent-accessible TPQ cofactor, although the true nature of substrate binding interactions within this enzyme remains unclear at this time. Furthermore, if the same TPQ_{amr}-4-(aryloxy)-2-butenal adduct observed in AGAO (Scheme 2) is responsible for inactivation of PPLO, it is not clear why it is resistant to either oxidation or hydrolysis (Scheme 3), given that it is most likely directly exposed to solvent. The observation of ~35% phenylhydrazine reactivity of the fully inhibited denatured PPLO may suggest a unique mode of inactivation for this enzyme.

The covalent modification of TPQ by **1** and **5** supports the lack of phenylhydrazine reactivity of fully inhibited samples of AGAO, as well as the fact that extensive dialysis did not result in any restoration of activity. However, it does not explain why full redox competency of the TPQ moiety, as indicated by the NBT assay, was restored when the inactivated enzymes were denatured. Two possible reaction mechanisms could explain the reversibility of inhibition observed upon enzyme denaturation (Scheme 3). Mechanism A involves the oxidation of the TPQ_{amr}-4-(aryloxy)-2-butenal moiety to a Schiff base which is then hydrolyzed in a similar manner as the TPQ_{imq} (Scheme 1, **F → A)** yielding TPQ_{ox} and 3-amino-4-(aryloxy)-2-butenal. In contrast to Mechanism A, where hydrolysis follows oxidation, Mechanism B involves an initial enamine hydrolysis (releasing 4-(aryloxy)-3-oxobutanal) followed by oxidation of the resulting TPQ_{amr}. The similar structural evidence obtained with compounds **1** and **5** in AGAO suggests that the same mechanisms for both inhibition and denaturation-dependent reversibility occur for all the 4-(aryloxy)-2-butynamine compounds studied (Schemes 2 and 3). A possible source for stabilization of the modified quinone in the native folded enzyme is the formation of a hydrogen bond between the aldehyde functional group of each TPQ-inhibitor adduct and the catalytic base (Figure 4). Such stabilization might protect the modified cofactor against the mechanisms proposed in Scheme 3.

The observation that the TPQ_{amr} species can itself act as an effective nucleophile in the covalent adduct formation described herein is unprecedented and suggests that the enzyme inactivation by other inhibitors turned over to electrophilic products may involve the TPQ cofactor rather than nucleophilic side-chains of the active site or substrate channel residues. Since the inactivation method defined here is a consequence of the inherent chemical reactivites of reduced TPQ and the aldehyde product, similar reactions with amine oxidases and lysyl oxidases may be involved in the physiological effects of toxic amines and aldehydes.

REFERENCES

1. Binda, C., Mattevi, A. and Edmondson, D. E. (2002) Structure−function relationships in flavoenzyme-dependent amine oxidations. A comparison of polyamine oxidase and monoamine oxidase, *J. Biol. Chem. 277*, 23973−23976.
2. Ruggiero, C. E. and Dooley, D. M. (1999) Stoichiometry of the topa quinone biogenesis reaction in copper amine oxidases, *Biochemistry 38*, 2892−2898.
3. Ruggiero, C. E., Smith, J. A., Tanizawa, K., and Dooley, D. M. (1997) Mechanistic studies of topa quinone biogenesis in phenylethylamine oxidase, *Biochemistry 36*, 1953−1959.
4. Molnar, J., Fong, K. S. K., He, Q. P., Hayashi, K., Kim, Y., Fong, S. F. T., Fogelgren, B., Szauter, K. M., Mink, A., and Csiszar, K. (2003) Structural and functional diversity of lysyl oxidase and the LOX-like proteins, *Biochim. Biophys. Acta Protein Struct. Mol. Enzymol. 1647*, 220−224.
5. Kagan, H. M., and Li, W. D. (2003) Lysyl oxidase: Properties, specificity, and biological roles inside and outside of the cell, *J. Cell. Biochem. 88*, 660−672.
6. Wilce, M. C. J., Dooley, D. M., Freeman, H. C., Guss, J. M., Matsunami, H., McIntire, W. S., Ruggiero, C. E., Tanizawa, K., and Yamaguchi, H. (1997) Crystal structures of the copper-containing amine oxidase from *Arthrobacter globiformis* in the holo and apo forms: Implications for the biogenesis of topaquinone, *Biochemistry 36*, 16116−16133.
7. Carter, S. R., McGuirl, M. A., Brown, D. E., and Dooley, D. M. (1994) Purification and active-site characterization of equine plasma amine oxidase, *J. Inorg. Biochem. 56*, 127−141.
8. Elmore, B., Bollinger, J. A., and Dooley, D. M. (2002) Human kidney diamine oxidase: Heterologous expression, purification, and characterization, *J. Biol. Inorg. Chem. 7*, 565−579.
9. McGuirl, M. A., McCahon, C. D., McKeown, K. A., and Dooley, D. M. (1994) Purification and characterization of pea seedling amine oxidase for crystallization studies, *Plant Physiol. 106*, 1205−1211.
10. McIntire, W. S., and Hartmann, C. (1993) Copper-Containing Amine Oxidases, in *Principles and Applications of Quinoproteins* (Davidson, V. L., Ed.) pp 97−171, Marcel Dekker, Inc. New York.
11. Mercier, N., Moldes, M., El Hadri, K., and Fève, B. (2003) Regulation of semicarbazide-sensitive amine oxidase expression by tumor necrosis factor-α in adipocytes: Functional consequences on glucose transport, *J. Pharmacol. Exp. Ther. 304*, 1197−1208.
12. Yu, P. H., Wright, S., Fan, E. H., Lun, Z. R., and Gubisne-Harberle, D. (2003) Physiological and pathological implications of semicarbazide-sensitive amine oxidase, *Biochim. Biophys. Acta 1647*, 193−199.
13. Boomsma, F., Bhaggoe, U. M., Van der Houwen, A. M. B., and Van den Meiracker, A. H. (2003) Plasma semicarbazide-sensitive amine oxidase in human (patho)physiology, *Biochim. Biophys. Acta Protein Struct. Mol. Enzymol. 1647*, 48−54.
14. Parsons, M. R., Convery, M. A., Wilmot, C. M., Yadav, K. D. S., Blakeley, V., Corner, A. S., Phillips, S. E. V., McPherson, M. J., and Knowles, P. F. (1995) Crystal structure of a quinoenzyme: Copper amine oxidase of *Escherichia coli* at 2 Å resolution, *Structure 3*, 1171−1184.
15. Kumar, V., Dooley, D. M., Freeman, H. C., Guss, J. M., Harvey, I., McGuirl, M. A., Wilce, M. C. J., and Zubak, V. M. (1996) Crystal structure of a eukaryotic (pea seedling) copper- containing amine oxidase at 2.2 Å resolution, *Structure 4*, 943−955.
16. Duff, A. P., Cohen, A. E., Ellis, P. J., Kuchar J. A., Langley, D. B., Shepard, E. M., Dooley, D. M., Freeman, H. C., and Guss, J. M. (2003) The crystal structure of *Pichia pastoris* lysyl oxidase, *Biochemistry 42*, 15148−15157.
17. Li, R. B., Klinman, J. P., and Mathews, F. S. (1998) Copper amine oxidase from *Hansenula polymorpha*: The crystal structure determined at 2.4 Å resolution reveals the active conformation, *Structure 6*, 293−307.
18. Dove, J. E., and Klinman, J. P. (2001) Trihydroxyphenylalanine quinone (TPQ) from copper amine oxidases and lysyl tyrosylquinone (LTQ) from lysyl oxidase, *Adv. Protein Chem. 58*, 141−174.
19. Dawkes, H. C., and Phillips, S. E. V. (2001) Copper amine oxidase: Cunning cofactor and controversial copper, *Curr. Opin. Struct. Biol. 11*, 666−673.
20. Halcrow, M., Phillips, S., and Knowles, P. (2000) Amine Oxidases and Galactose Oxidase, in *Subcellular Biochemistry* (Holzenburg, A., Scrutton, N., Eds.) pp 183−231, Kluwer Academic/Plenum Publishers, New York.
21. Shepard, E. M., Smith, J., Elmore, B., Kuchar J. A., Sayre, L. M., and Dooley, D. M. (2002) Towards the development of

selective amine oxidase inhibitors. Mechanism-based inhibition of six copper containing amine oxidases, *Eur. J. Biochem. 269*, 3645−3658.

22. Murray, J. M., Saysell, C. G., Wilmot, C. M., Tambyrajah, W. S., Jaeger, J., Knowles, P. F., Phillips, S. E. V., and McPherson, M. J. (1999) The active site base controls cofactor reactivity in *Escherichia coli amine* oxidase: X-ray crystallographic studies with mutational variants, *Biochemistry 38*, 8217−8227.
23. Wilmot, C. M., Murray, J. M., Alton, G., Parsons, M. R., Convery, M. A., Blakeley, V., Corner, A. S., Palcic, M. M., Knowles, P. F., McPherson, M. J., and Phillips, S. E. V. (1997) Catalytic mechanism of the quinoenzyme amine oxidase from *Escherichia coli*: Exploring the reductive half-reaction, *Biochemistry 36*, 1608−1620.
24. Mure, M., Mills, S. A., and Klinman, J. P. (2002) Catalytic mechanism of the topa quinone containing copper amine oxidases, *Biochemistry 41*, 9269−9278.
25. Mills, S. A. and Klinman, J. P. (2000) Evidence against reduction of Cu2+ to Cu+ during dioxygen activation in a copper amine oxidase from yeast, *J. Am. Chem. Soc. 122*, 9897−9904.
26. Mills, S. A., Goto, Y., Su, Q. J., Plastino, J., and Klinman, J. P. (2002) Mechanistic comparison of the cobalt-substituted and wild-type copper amine oxidase from *Hansenula polymorpha*, *Biochemistry 41*, 10577−10584.
27. Schwartz, B., Olgin, A. K., and Klinman, J. P. (2001) The role of copper in topa quinone biogenesis and catalysis, as probed by azide inhibition of a copper amine oxidase from yeast, *Biochemistry 40*, 2954−2963.
28. Abeles, R. H. and Maycock, A. L. (1976) Suicide enzyme inactivators, *Acc. Chem. Res. 8*, 313−319.
29. Neumann, R., Hevey, R., and Abeles, R. H. (1975) Action of plasma amine oxidase on beta-haloamines. Evidence for proton abstraction in the oxidative reaction, *J. Biol. Chem. 250*, 6362−6367.
30. Hevey, R. C., Babson, J., Maycock, A. L., and Abeles, R. H. (1973) Highly specific enzyme inhibitors. Inhibition of plasma amine oxidase, *J. Am. Chem. Soc. 95*, 6125−6127.
31. Tang, S. S., Simpson, D. E., and Kagan, H. M. (1984) Beta-substituted ethylamine derivatives as suicide inhibitors of lysyl oxidase, *J. Biol. Chem. 259*, 975−979.
32. Kumagai, H., Uchida, H., and Yamada, H. (1979) Reaction of fungal amine oxidase with beta-bromoethylamine, *J. Biol. Chem. 254*, 10913−10919.
33. Medda, R., Padiglia, A., Pedersen, J. Z., Agro, A. F., Rotilio, G., and Floris, G. (1997) Inhibition of copper amine oxidase by haloamines: A killer product mechanism, *Biochemistry 36*, 2595−2602.
34. Pino, R. and Lyles, G. A. (1997) Effect of activity of semicarbazide-sensitive aminooxidases and cellular glutathione on the cytotoxic effect of allylamine, acrolein, and formaldehyde in human cultured endothelial cells, *Vopr. Med. Khim. 43*, 537−547.
35. Blicharski, J. R. and Lyles, G. A. (1990) Semicarbazide-sensitive amine oxidase activity in rat aortic cultured smooth muscle cells, *J. Neural Transm. Suppl. 32*, 337−339.
36. Yu, P. H., Davis, B. A., and Boulton, A. A. (1995) Aliphatic propargylamines, a new series of potent selective, irreversible nonamphetamine-like MAO−B inhibitors. Their structures, function and pharmacological implications, *Adv. Exp. Med. Biol. 363*, 17−23.
37. Abeles, R. H. and Tashjian, A. H., Jr. (1975) Comparison of the inhibitory effects of propargylamine and pargyline on brain and liver monoamine oxidase activity, *Biochem. Pharmacol. 24*, 307−308.
38. Boulton, A. A., Davis, B. A., Durden, D. A., Dyck, L. E., Juorio, A. V., Li, X. M., Paterson, I. A., and Yu, P. H. (1997) Aliphatic propargylamines: New antiapoptotic drugs, *Drug Dev. Res. 42*, 150−156.
39. Kuchar J. A. (2001) Cloning, sequence analysis, and characterization of the "Lysyl Oxidase" from *Pichia pastoris*, Ph.D. Thesis, Montana State University, Bozeman.
40. Elmore, B. O. (2002) Characterization of recombinant human kidney diamine oxidase and equine plasma amine oxidase, Ph.D. Thesis, Montana State University, Bozeman.
41. Janes, S. M. and Klinman, J. P. (1991) An investigation of bovine serum amine oxidase active site stoichiometry: Evidence for an aminotransferase mechanism involving two carbonyl cofactors per enzyme dimer, *Biochemistry 30*, 4599−4605.
42. Juda, G. A., Bollinger, J. A., and Dooley, D. M. (2001) Construction, overexpression, and purification of *Arthrobacter globiformis* amine oxidase − *Strep*-Tag II fusion protein, *Protein Expr. Purif. 22*, 455−461.
43. Jeon, H. B., Sun, G., and Sayre, L. M. (2003) Inactivation of bovine plasma amine oxidase by 4-aryloxy-2-butynamines and related analogues, *Biochim. Biophys. Acta Protein Struct. Mol. Enzymol. 1647*, 343−354.
44. Kuchar, J. and Dooley, D. (2001) Cloning, sequence analysis, and characterization of the "Lysyl Oxidase" from *Pichia pastoris*, *J. Inorg. Biochem. 83*, 193−204.
45. Suzuki, S., Sakurai, T., Nakahara, A., Manabe, T., and Okuyama, T. (1983) Effect of metal substitution on the chromophore of bovine serum amine oxidase, *Biochemistry 22*, 1630−1635.
46. Tabor, C. W., Tabor, H., and Rosenthal, S. M. (1954) Purification of amine oxidase from beef plasma, *J. Biol. Chem. 208*, 645−661.
47. Szutowicz, A., Kobes, R. D., and Orsulak, P. J. (1984) Colorimetric assay for monoamine oxidase in tissues using peroxidase and 2, 2′-azinodi(3-ethylbenzthiazoline-6-sulfonic acid) as chromogen, *Anal. Biochem. 138*, 86−94.
48. Segal, I (1976) *Biochemical Calculations*, 2nd ed., John Wiley & Sons, New York.
49. Otwinowski, Z. and Minor, W. (1997) *Methods Enzymol. 267*, 307−326.
50. Leslie, A. G. W. (1992) in Joint CCP4+ESF-EAMCB Newsletter on Protein Crystallography, 26.
51. Evans, P. R., Sawyer, L., Isaacs, N., and Bailey, S. (1994) The CCP4 suite: Programs for protein crystallography, *Acta Crystallogr. D53*, 760−763.
52. Murshudov, G. N., Vagin, A. A., and Dodson, E. J. (2004) Refinement of macromolecular structures by the maximum-likelihood method, *Acta Crystallogr.* 240−255.
53. Lamzin, V. S. and Wilson, K. S. (1993) Automated refinement of protein models, *Acta Crystallogr., Sect. D 49*, 129−149.
54. Jones, T. A., Zou, J. Y., Cowan, S. W., and Kjeldgaard (2004) Improved methods for building protein models in electron density maps and the location of errors in these models, *Acta Crystallogr., Sect. A 47*, 110−119.
55. van Aalten, D. M. F., Bywater, R., Findlay, J. B. C., Hendlich, M., Hooft, R. W. W., and Vriend, G. (1996) PRODRG, a program for generating molecular topologies and unique molecular descriptors from coordinates of small molecules, *J. Comput. Aided Mol. Des. 10*, 255−262.
56. Lovell, S. C., Davis, I. W., Arenda, W. B., III, de Bakker, P. I. W., Word, J. M., Prisant, M. G., Richardson, J. S., and Richardson, D. C. (2003) Structure validation by C-alpha geometry: phi, and C-beta deviation, *Proteins: Struct., Funct., Genet. 50*, 437−450.
57. Laskowski, R. A., MacArthur, M. W., Moss, D. S., and Thornton, J. M. (1993) PROCHECK: a program to check the stereochemical quality of protein structures, *J. Appl. Crystallogr. 26*, 283−291.
58. Silverman, R. B. (1988) Mechanism Based Enzyme Inactivation, pp 3−30, CRC Press, Inc., FL.
59. De Biase, D., Agostinelli, E., De Matteis, G., Mondovi, B., and Morpurgo, L. (1996) Half-of-the-sites reactivity of bovine serum amine oxidase − Reactivity and chemical identity of the second site, *Eur. J. Biochem. 237*, 93−99.
60. Frebort, I., Toyama, H., Matsushita, K., and Adachi, O. (1995) Half-site reactivity with *p*-nitrophenylhydrazine and subunit separation of the dimeric copper-containing amine oxidase from *Aspergillus niger*, *Biochem. Mol. Biol. Int. 36*, 1207−1216.
61. Kim, M., Okajima, T., Kishishita, S., Yoshimura, M., Kawamori, A., Tanizawa, K., and Yamaguchi, H. (2002) X-ray snapshots of quinone cofactor biogenesis in bacterial copper amine oxidase, *Nature Struct. Biol. 9*, 591−596.
62. Jeon, H. B. and Sayre, L. M. (2003) Highly potent propargylamine and allylamine inhibitors of bovine plasma amine oxidase, *Biochem. Biophys. Res. Commun. 304*, 788−794.
63. Jeon, H. B., Lee, Y., Qiao, C., Huang, H., and Sayre, L. M. (2003) Inhibition of bovine plasma amine oxidase by 1,4-diamino-2-butenes and −2-butynes, *Bioorg. Med. Chem. 11*, 4631−4641.
64. Lee, Y., Ling, K. Q., Lu, X. L., Silverman, R. B., Shepard, E. M., Dooley, D. M., and Sayre, L. M. (2002) 3-Pyrrolines are mechanism-based inactivators of the quinone-dependent amine

oxidases but only substrates of the flavin-dependent amine oxidases, *J. Am. Chem. Soc. 124*, 12135−12143.
65. Frebort, I., Pec, P., Luhova, L., Matsushita, K., Toyama, H., and Adachi, O. (1994) Active-site covalent modifications of quinoprotein amine oxidases from *Aspergillus niger*-Evidence for binding of the mechanism-based inhibitor, 1,4-diamino-2-butyne, to residue Lys356 involved in the catalytic cycle, *Eur. J. Biochem. 225*, 959−965.
66. Frebort, I., Sebela, M., Svendsen, I., Hirota, S., Endo, M., Yamauchi, O., Bellelli, A., Lemr, K., and Pec, P. (2000) Molecular mode of interaction of plant amine oxidase with the mechanism-based inhibitor 2-butyne-1,4-diamine, *Eur. J. Biochem. 267*, 1423−1433.
67. Matsuzaki, R., and Tanizawa, K. (1998) Exploring a channel to the active site of copper/topaquinone- containing phenylethylamine oxidase by chemical modification and site-specific mutagenesis, *Biochemistry 37*, 13947−13957.

BI0492004